Supplementary Information

Probing membrane hydration in microfluidic polymer electrolyte membrane electrolyzers via operando synchrotron Fouriertransform infrared spectroscopy

Kevin Krause[1], Marine Garcia[1], Dominique Michau[2], Gérald Clisson[3], Brant Billinghurst[4], Jean-Luc Battaglia[1], Stéphane Chevalier[1]

[1] Arts et Métiers Institut de Technologie, CNRS, Université de Bordeaux, Bordeaux INP Institut de mécanique et d'ingénierie (I2M), Bâtiment A11, 351 Cours de la Libération, 33405 Talence, France

[2] Université de Bordeaux, CNRS, Bordeaux INP Institut de Chimie de la Matière Condensée de Bordeaux (ICMCB) F-33600 Pessac, France

[3] Solvay, LOF, UMR 5258, CNRS, Université de Bordeaux 33600 Pessac, France

[4] Canadian Light Source Far-Infrared Beamline, 44 Innovation Blvd, Saskatoon, SK S7N 2V3, Canada

Membrane break in

The proton exchange membrane (PEM) was broken in for the assembled electrolyzer using an alternating constant voltage script to improve its performance. The procedure was inspired by the procedure written by Klug.[1] The script cycles the PEM electrolyzer through potentiostatic operation at 2 V, 2.25 V, then 2.5 V for 1 min each and repeating for 20 cycles (total time of 1 hour). At the beginning of break-in script and at a potential of 2.5 V, the chip was consistently achieving 3 mA cm^{-2}, and at the end of the break-in script the chip achieved 6.25 mA cm^{-2} at the same potential.

Raw Infrared Spectra

The raw infrared (IR) transmission spectra acquired during the Fourier transform IR (FTIR) spectroscopy are cropped around the peak of interest. The peak of interest is roughly centered around a wavelength of 10.7 μm and is the only observable peak in the measured spectrum where water attenuated the beam. The IR spectra are averaged for 300 acquisitions with a spectral resolution of 4 cm^{-1}. Each acquisition is measured during the final two minutes of steady current operation and results are presented for all experimental conditions.

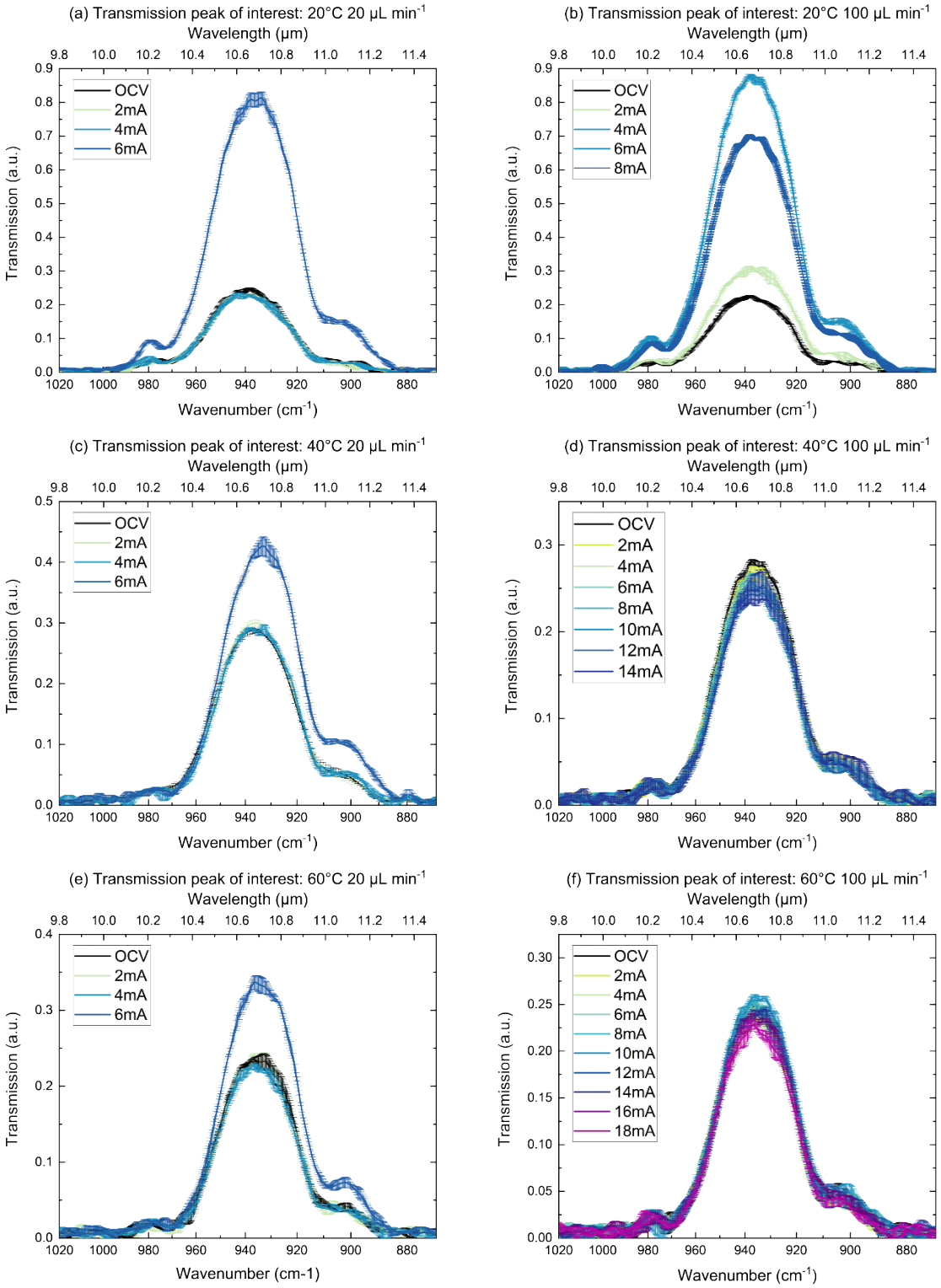

Fig. S1: Averaged IR spectra from 300 acquisitions for each constant current operating condition for (a) 20 °C, 20 µL min^{-1}, (b) 20 °C, 100 µL min^{-1}, (c) 40 °C, 20 µL min^{-1}, (d) 40 °C, 100 µL min^{-1}, (e) 60 °C, 20 µL min^{-1}, and (f) 60 °C, 100 µL min^{-1}.

Determining the beam size

The beam diameter is determined by assuming a Gaussian beam and performing a knife-edge measurement. By using the interface in the channel of the chip and the edge of the electrodes, a sharp edge representing a knife-edge can be obtained for the necessary measurements. The methodology for determining the beam size analysis is performed by Kirkham and is replicated here.[2] The final beam radius is determined to be 45.62 ± 0.48 µm for a wavelength of 10.7 µm.

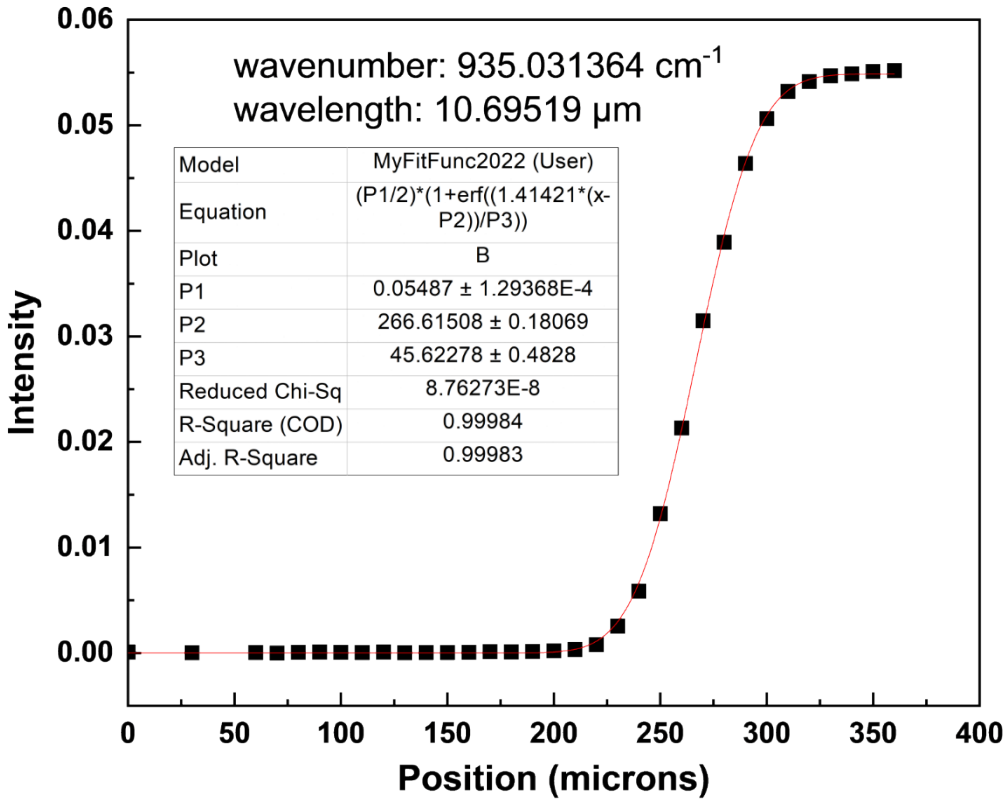

Fig. S2: The resulting error function plot with fitting parameters P1, P2, and P3 for a wavelength of 10.7 µm. P3 corresponds to $1/e^2$ radius of the Gaussian beam, where the calculated beam radius is 45.62278 ± 0.4828 µm.

Electrochemical impedance spectroscopy

Ohmic resistance measurements extracted from electrochemical impedance spectroscopy (EIS) are challenging to obtain for the proposed cell geometry due to its small active area of 0.08 cm^2. To improve the accuracy of ohmic resistance measurements, an impedance model from the work presented by Chevalier et al. is applied onto the experimentally obtained Nyquist plots, and the ohmic resistance was extracted.[3] A sample Nyquist plot with the fitted model is shown in Figure S3. Individual ohmic resistance measurements and the corresponding ohmic voltage losses are graphically reported in Figure S4 for each operating condition. Ohmic voltage losses are computed through the following equation:

$$\eta_{ohmic} = iR_{ohmic} \quad \text{[Eq. S1]}$$

where η_{ohmic} are the ohmic voltage losses (V), i is the current density (mA cm^{-2}), and R_{ohmic} is the ohmic resistance (Ω cm^2).

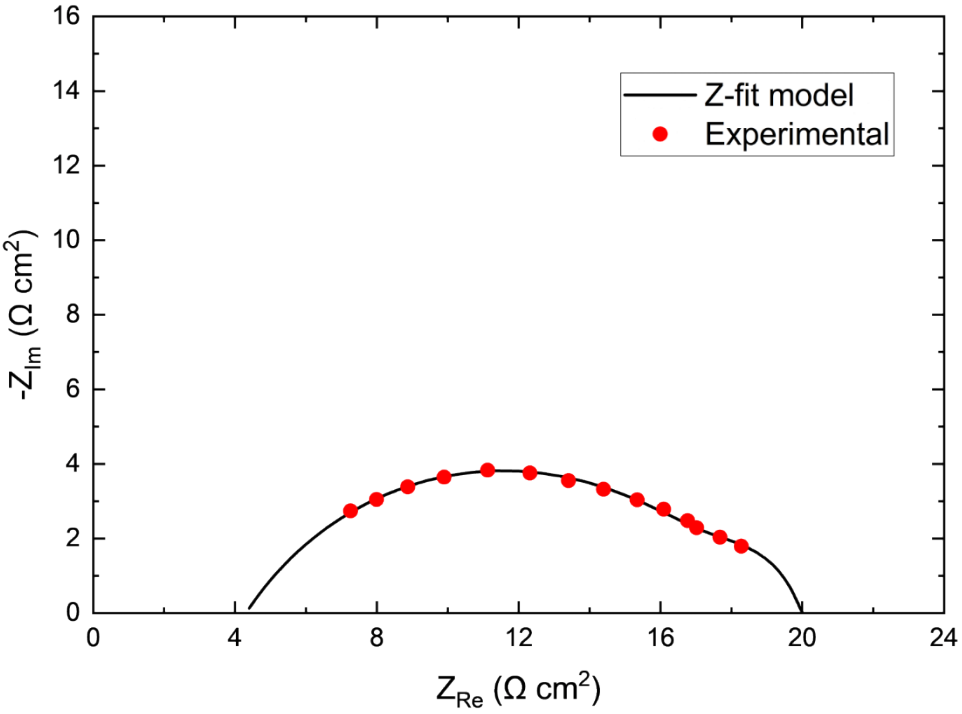

Fig. S3: A sample Nyquist plot with the corresponding Z-fit model obtained at 20 °C with a flow rate of 20 µL min^{-1} and at a current density of 30 mA cm^{-2}. The extracted ohmic resistance is 4.31 Ω cm^2 and can be seen in Figure S5 as well.

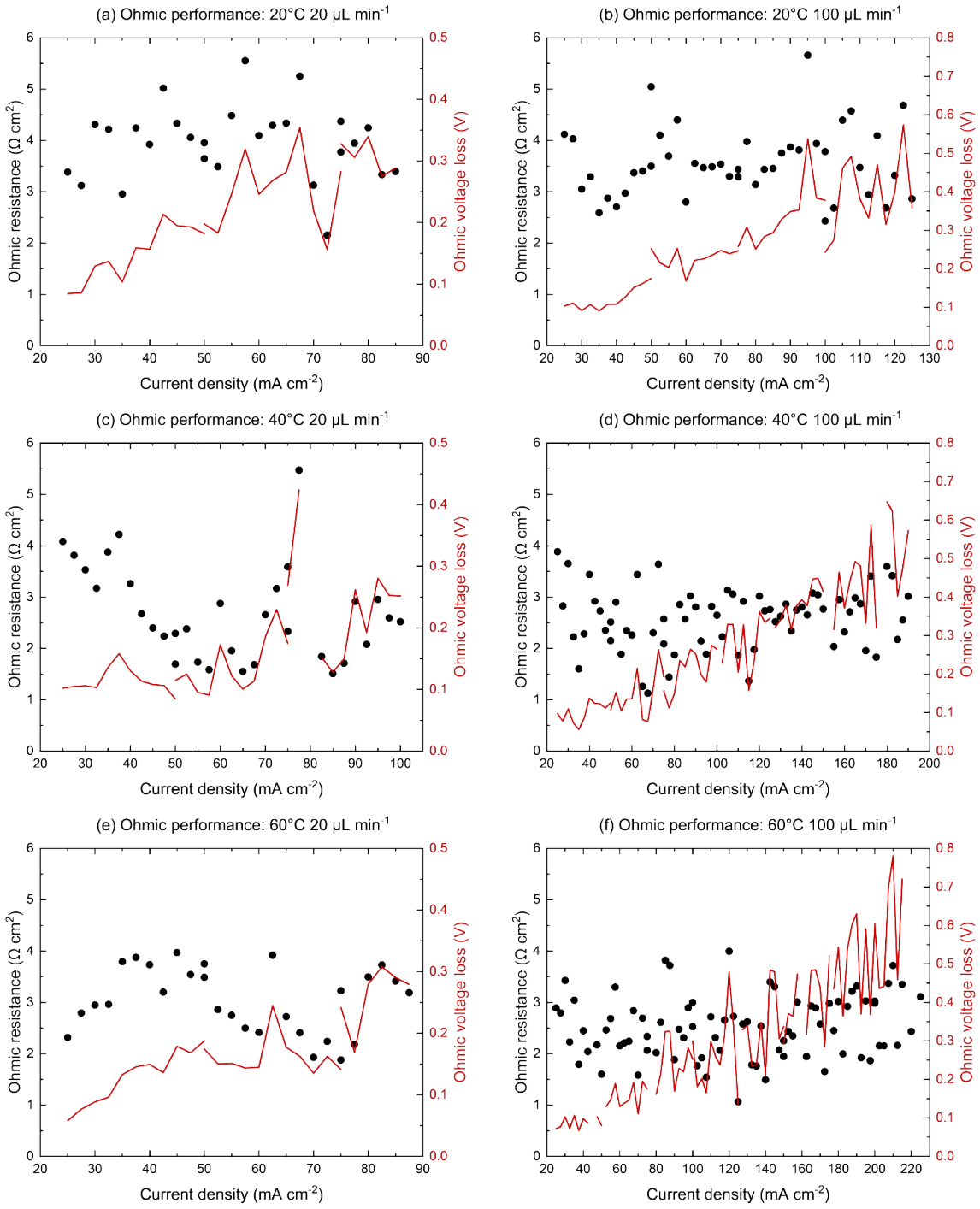

Fig. S4: Measured ohmic resistance acquired from imposing a Z-fit onto experimentally acquired SGEIS data and the corresponding ohmic voltage losses for (a) 20 °C, 20 µL min^{-1}, (b) 20 °C, 100 µL min^{-1}, (c) 40 °C, 20 µL min^{-1}, (d) 40 °C, 100 µL min^{-1}, (e) 60 °C, 20 µL min^{-1}, and (f) 60 °C, 100 µL min^{-1}.

Water attenuation coefficient

The attenuation coefficient for water μ_w is determined based on the transmission data for 1 µm of liquid water at room temperature (25 °C) published by Hale and Querry, which is also available on the Refractive index database for enhanced convenience.[4,5] The change in the transmission of water is neglected for higher temperatures, as changes in the thermal transmission coefficient can be on the order of 10^{-3} K^{-1}.[6] Specifically, their transmission data was interpolated for the cropped wavelength range [9.8 µm - 11.5 µm] through the following binomial fit:

$$T_w = -0.026x^2 + 0.504x - 1.497 \quad \text{[Eq. S2]}$$

Where T_w is the transmission of water and x is the wavelength of light being transmitted. In Figure S5, a comparison between the binomial fit and experimental data published by Hale and Querry is shown.[4,5] The transmission for 1 µm of water is then converted to the absorbance per µm of water (μ_w [μm^{-1}]) through the following negative base 10 logarithmic function.

$$\mu_w = -\log_{10}\left(\frac{T_w}{100\%}\right) \quad \text{[Eq. S3]}$$

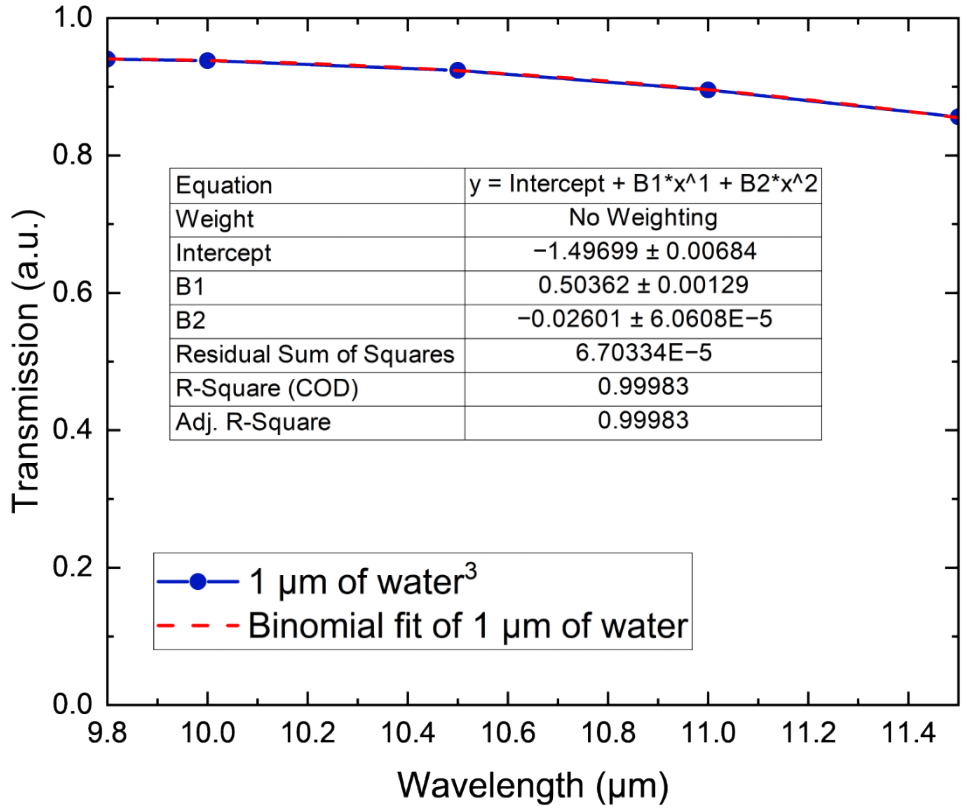

Fig. S5: The transmittance of 1 µm of water according to the data published by Hale and Querry in comparison to the applied binomial fit from Equation S2, cropped over the wavelength range of [9.8 µm - 11.5 µm].[4]

References:
1 Sarah Klug, 2021, 1–6.
2 D. Kirkham, 2016.
3 S. Chevalier, N. Ge, J. Lee, M. G. George, H. Liu, P. Shrestha, D. Muirhead, N. Lavielle, B. D. Hatton and A. Bazylak, *J. Power Sources*, 2017, **352**, 281–290.
4 G. M. Hale and M. R. Querry, *Appl. Opt.*, 1973, **12**, 555.
5 M. N. Polyanskiy, Refractive index database, https://refractiveindex.info, (accessed 29 June 2023).
6 C. Bourges, S. Chevalier, J. Maire, A. Sommier, C. Pradere and S. Dilhaire, 2022, 1–16.